

Supplementary materials:

Flow-cytometry analysis:

A BD Accuri™ C6 plus cell cytometer with 488nm and 640nm excitation lasers was used for all flow cytometry analysis according to the manufacturer's standard protocols (BD Biosciences, San Jose, CA). Colon cancer cell lines were analyzed by flow for expression of pAKT473, pAKT308, Rictor, VEGF, CD44, CD133, and Lgr5 following respective antibody staining protocols provided by the manufacturer (BD Biosciences). Data was analyzed using FlowJo v10.8 (BD Biosciences).

xCELLigence real-time cell analysis:

Cell migration, invasion, and adhesion assays in real-time were performed using xCELLigence technology, as previously described (1). GraphPad Prism (version 9) was used to analyze the rate of cell proliferation, migration, and invasion (slope) during a critical time window for the HCT-116 cell line in 10% FBS-McCoy. Cells were pre-treated with vehicle or VTD (100mM). 2×10^4 cells were loaded into E-Plat (proliferation assay) as well as the upper chamber of CIM-plate without Matrigel (migration) or with Matrigel (invasion) in the presence of 1% FBS-McCoy media (starved media). The xCELLigence system measured the impedance value of each well every 15 minutes for 120 hours which is expressed as a CI value for cell proliferation, migration, and invasion. We used plots to illustrate the Cell index value for overtime points. The critical time point for cell proliferation was approximately between 10 hours to 20 hours. For migration, the critical time point was approximately between 30 hours to 50 hours after starting the experiments.

Cell culture

We purchased the colon cancer cells used in this study (HCT-116, SW480, SW620, LoVo) from American Type Culture Collection (VA, USA) and grew them in the recommended medium. All examined cell lines were in passages limited to 10 and, per the manufacturer's protocol, were routinely checked for mycoplasma contamination using the PCR Mycoplasma Detection Kit (Applied Biological Materials (abm)-USA). We constructed the CRISPR expression plasmids against UBXN2A, followed by the generation of a stable pool of HCT-116 cells, using 0.5 $\mu\text{g/ml}$ puromycin for two days. Genotyping followed by WB demonstrated two successful UBXN2A knockout HCT-cells lines, which were used for conducted experiments. For the rescue experiments, we used an MYC-Rictor mammalian vector (ID: 11367). The pCMV6-Kana/Neo vector (#RC210524, DDK-tagged ORF clone of Homo sapiens UBX domain protein 2A (UBXN2A:#NM_181713) was purchased from Origene. MYC-Empty and DDK Empty plasmids were used for control cells. We used DharmaFECT kb DNA transfection reagent (#T-2006-01-Horizon) for DDK-UBXN2A transfection to cancer cells using the protocol provided by the manufacturer. We used FuGENE® 4K Transfection Reagent (Promega) for transient transfection in rescue experiments using the protocol provided by the manufacturer.

Organoid culture and treatment.

Human patient-derived organoids were obtained from the Organoid Core in the Organoids of the Nebraska Center for Molecular Target Discovery and Development and Buffett Cancer Center at UNMC. Organoids were maintained embedded in reduced growth factor basement membrane extract, Type 2 (BME) (R&D Systems) in organoid culture medium (Advanced DMEM/F12 containing 20% R-Spondin conditioned medium, 10% Noggin conditioned medium, 1 x B27 supplement, 10 mM nicotinamide, 1.25 mM N-acetylcysteine, 100 $\mu\text{g/ml}$ Primocin®, 50 ng/ml epidermal growth factor (EGF), 3 μM SB202190, 0.5 μM A83-01, 1 μM prostaglandin E2) as described (2). Immediately following the passage, the medium was supplemented with 10 μM Y-

27632. For drug treatments, cells were suspended in an organoid culture medium supplemented with Y-27632 and containing 5% (v/v) BME. Following treatment for the indicated times, organoids were rinsed 2 x with ice-cold phosphate-buffered saline prior to analysis.

Cancer Cells for Xenografts

The HCT-116 cell line used for the apoptosis assay was obtained from the ATCC (American Type Culture Collection). HCT-116 iRFP cell line was purchased from Lmanis life science (USA). HCT-116 cells were cultured in McCoy's 5A Medium supplemented with 10% fetal bovine serum and penicillin/streptomycin. Low passages (2 to 5) were used for apoptosis experiments. For the xenograft experiments, HCT-116 iRFP (passage 4) at 70% confluence were incubated with Accutase cell detachment solution (BD Biosciences) for 3min. After centrifugation (2500rpm, 3min), dead cells and debris were removed by two-times wash with ice-cold PBS. Cells were suspended in Hanks' balanced salt solution without sodium, magnesium, and phenol red (Alfa Aesar, USA) and counted.

RT-PCR and Western Blot

60mg of colon tissue was subsequently prepared and placed in a digitonin lysis buffer (50mM Tris/HCl, pH 7.5, 150mM NaCl, 1% Digitonin (Sigma-Aldrich, St. Louis, MO) plus 1x mammalian complete protease inhibitor (Research Products International Corp). Silicon/Zirconia Beads 2.3mm were then added to the tube containing the lysis buffer, and cells were mechanically homogenized for 30s with the MiniBead Beater (Biospec Products). Following homogenization, tissue lysates were centrifugated at 13 000rpm for 10min at 4°C, and the supernatant was moved to a fresh Eppendorf tube in preparation for Western Blot (WB). Cell lysates used in WB were normalized for equal loading by NanoDrop using direct absorbance at 280nm (ThermoFisher Scientific). Samples were loaded onto SDS-PAGE 4-20% gradient gel. Protein transfer was performed using an iBlott 2 system for probing with the corresponding antibodies. We used a homemade anti-UBXN2A rabbit polyclonal to detect UBXN2A in tissue lysates (Table 2, Supplemental Materials)(2)WB membranes were scanned using the LI-COR Odyssey CLx (LI-COR Biosciences, Lincoln, NE, USA) using fluorescent secondary antibodies and images were evaluated using Image Studio v5.2 software. WB and ELISA experiments were performed in triplicate except when otherwise noted and represented as mean \pm SD. FACS experiments were performed in quadruplets and represented as mean \pm SD. Pull-down and ubiquitination assays were conducted in duplicate.

Assessment of apoptosis

HCT-116 cells were treated with different concentrations of VTD (10, 30, 100mM) for 48h. DMSO at a concentration of 0.01% was used as a control. Early and late apoptosis in cells was assessed using a Propidium iodide (PI)/Annexin V Apoptosis Detection Kit (BD Pharmingen) analyzed by a BD Accuri C6 flow cytometer according to the manufacturer's instructions. Ten thousand gated events were collected per sample. Experiments were conducted in triplicate.

UBXN2A affects survival analysis in COAD, READ, and CRC

We used two interactive survival analysis online tools (Human protein atlas and www.oncolnc.org) to perform UBXN2A survival analysis in COAD, READ, and CRC. The human protein atlas contains 3 sets of datasets: 1) RNA-seq tissue data in mean transcripts per million from HPA, 2) RNA-seq data in median reads per kilobase per million mapped reads from the GTEx dataset, and 3) cap analysis gene expression in tags per million data from FANTOM5

dataset. OncoLnc contains data from 8647 patients on 21 cancer studies from the Cancer Genome Atlas (TCGA). The Kaplan-Meier plots were created based on specific gene (UBXN2A) expression levels among the subjects in these datasets. Furthermore, to assess UBXN2A's prognostic marker indicative, cox-regression analysis was performed. The results show that in COAD, UBXN2A could be a predictive marker supported by a Cox Coefficient of -0.149 (A negative Cox Coefficient suggests a significant prognostic marker) and a P-Value of 1.40e-01. In READ, the opposite is true, supported by the Cox Coefficient of 0.147 (positive Cox Coefficient suggests possible non-marker) and P-Value of 4.80e-01 (3, 4).

COAD	READ
Cox Coefficient: -0.149 (negative suggests Significant prognostic marker) P-Value: 1.40e-01 FDR: 5.42e-01 Rank: 4226 Median Expression: 257.28 Mean Expression: 263.18	Cox Coefficient: 0.147 (positive suggest not) P-Value: 4.80e-01 FDR: 9.67e-01 Rank: 8180 Median Expression: 242.36 Mean Expression: 250.45

Table 1: **Cox regression results for UBXN2A**

Patient-derived xenografts

The tissues extracted from CRC patient-derived xenografts and their clinical information were provided by Dr. Michael Linnebacher (5).

Statistical analysis using GraphPad Prism

We observed a variation within the group or between groups in animal experiments. These variations were calculated in ANOVA from the sum of squares (SS), and this value is given in ANOVA test results using GraphPad Prism software. We did not observe any warning in the presented data in this study. When we had two groups to be compared, for example, animal groups in Figure 1 and Figure 2, we used the F-test to test if the variances of the two populations were equal. Then we used one- or two-tailed tests.

Name	Manufacturer and Catalog Number	Dilution	Catalog number
Rabbit polyclonal anti-UBXN2A against #C-IQRLQKTASFRELS peptide located in the c-terminus of human UBXN2A	Pacific Immunology Corp	1:1000 (WB)	-
Living Colors® A.v. Monoclonal Antibody (JL-8)	Clontech-Takara	1:1000 (WB)	632380
Anti-Green Fluorescent Protein, Polyclonal antibody	Millipore	1:1000 (WB)	AB3080
Phospho-Akt (Ser473) (D9E) XP® Rabbit mAb	Cell Signaling	1: 500 (WB)	4060T
Phospho-Akt (Thr308) (D25E6) XP® Rabbit mAb	Cell Signaling	1: 500 (WB)	13038T
Anti-Akt1 Antibody (B-1)	Santa Cruz Biotechnology, Inc.	1: 500 (WB)	sc-5298
mTOR Rabbit Polyclonal antibody	Proteintech Group Inc	1: 500 (WB)	#20657-1-AP
RICTOR Rabbit Poly Ab and Rictor monoclonal	Proteintech Group Inc	1: 500 (WB)	#27248-1-AP and 66867-2-Ig
Beta Tubulin Mouse Monoclonal antibody, Cat No.	Proteintech Group Inc	1:2000 (WB)	66240-1-Ig
GAPDH Mouse Monoclonal antibody, Catalog Number	Proteintech Group Inc	1:2000 (WB)	# 60004-1-Ig
AKT 473 was Phospho-Akt (Ser473) (D9E) XP® Rabbit mAb (Alexa Fluor® 647 Conjugate)	Cell Signaling	3-5 µl/10 ⁶ cells	4075
Phospho-Akt (Thr308) (D25E6) XP® Rabbit mAb (Alexa Fluor® 647 Conjugate)	Cell Signaling	3-5 µl/10 ⁶ cells	48646
E-Cadherin (24E10) Rabbit mAb	Cell Signaling	1: 1000 (WB)	3195T
PRAS40 (D23C7) XP® Rabbit mAb	Cell Signaling	1: 1000 (WB)	2691
Phospho-PRAS40 (Thr246) (D4D2) XP® Rabbit mAb	Cell Signaling	1: 500 (WB)	13175
Phospho-p70 S6 Kinase (Thr389) Antibody	Cell Signaling	1: 500 (WB)	9205
PARP Antibody and Cleaved PARP (ASP214) antibody (human Specific)	Cell Signaling	1: 500 (WB)	9542 and 9541
Mono- and polyubiquitinated conjugates monoclonal antibody (FK2)	Enzo	1:2000 (WB)	BML-PW1210-0025
Caspase-3 (8G10) Rabbit mAb	Cell Signaling	1: 500 (WB)	9665
Bax (YTH6A7)	Santa Cruz Biotechnology, Inc.	1: 500 (WB)	sc-80658

Mouse anti-Glyceraldehyde-3-Phosphate Dehydrogenase antibodies (anti-GAPDH, loading controls, and cytoplasmic marker).	Millipore	1:20000	ZRB374
Human/Mouse/Rat p70 S6 Kinase Alexa Fluor® 488-conjugated Antibody	Bio-Techne	5 µl/10 ⁶ cells	IC8962G
Human/Mouse/Rat p70 S6 Kinase PE-conjugated Antibody	Bio-Techne	10 µl/10 ⁶ cells	IC8962P
IRDye 800CW Goat anti-Rabbit IgG (H+L),	LI-COR Corporate	1:3000	827-08365
IRDye 680LT anti-Rabbit IgG (H+L)	LI-COR Corporate	1:3000	926-68023
Anti-DDK (FLAG) monoclonal antibody	OriGene	1: 2000	TA50011-100
Human BD Fc Block	BD Pharmingen	1 µl/10 ⁶ cells	564220
Ms IgG2b Kpa PE	BD Pharmingen	1 µl/10 ⁶ cells	555743
PE Mouse Anti-Human CD44	BD Pharmingen	1 µl/10 ⁶ cells	561858
APC Mouse Anti-Human CD133	BD Pharmingen	1 µl/10 ⁶ cells	566597
APC Mouse IgG1 k Isotype Control	BD Pharmingen	1 µl/10 ⁶ cells	554681
Alexa Flour 647 Rat IgG2b, k Isotype Control	BD Pharmingen	1 µl/10 ⁶ cells	557691
Mouse Monoclonal VEGF Antibody (VG1) [Allophycocyanin]	Novus Biologicals and biotechne brand	2.5 µl/10 ⁶ cells	NB100-664APC
Myc-Tag Antibody	Cell signaling	1/500	#2272
Anti-vimentin	Santa Cruz Biotechnology, Inc.	1/500	sc-373717

Table 2: This table lists antibodies and their dilutions used in this study.

Synthego quality control for CRISPR UBXN2A Ko cells.

Tube	Label	Guide Sequence	# Cells / Yield
1	UBXN2A-23971310 Knockout - LOVO p2	GAUUGUUGAUUAAUACCAAG	10 ⁶ cells
2	UBXN2A-23971310 Knockout - LOVO p2	GAUUGUUGAUUAAUACCAAG	10 ⁶ cells
3	LOVO WT p2	None	10 ⁶ cells
4	LOVO WT p2	None	10 ⁶ cells

For information on how to thaw your Engineered Cells, please see our [Quick Start Guide](#).

UBXN2A-23971310 Knockout cells

Guide RNA sequence: GAUUGUUGAUUAAUACCAAG

LOVO p2

Transcript ID: ENST00000309033 Exon Targeted: Exon 3

PCR and Sequencing Primers:

F: GCACAGGACACCTCATACAG

R: CTCGATCTTAGCCCACTGCAACCTC

GC enhancer used? No

Analysis

Assay	LOVO Parental Line (WT)	LOVO UBXN2A-23971310 KO Cell Pool
48-hrs Post-Transfection Editing Efficiency	N/A	90.00%
Editing Efficiency After Expansion	N/A	85.00%

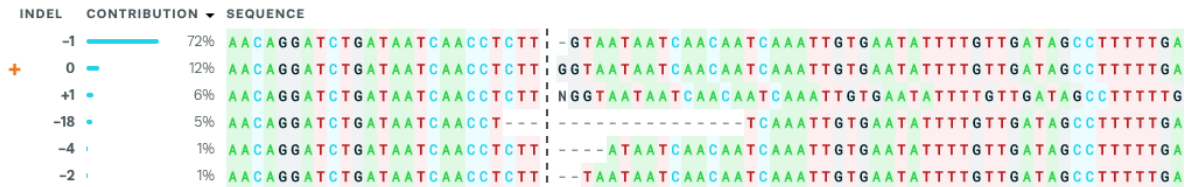
Post-thaw Viability	Pass (82.10%)	Pass (95.00%)
Mycoplasma Test	Negative	Negative
Passage	2	2

No sign of microbiological contamination was observed.

Status [?]  Succeeded <small>Padding alignment window to be at least 40bp in length or to start of seq</small>	Guide Target [?] GATTGTTGATTATTACCAAG	PAM Sequence [?] AGG	Indel % [?] 85	Model Fit (R²) [?] 0.97	Knockout-Score [?] 80
--	---	--	--	--	---

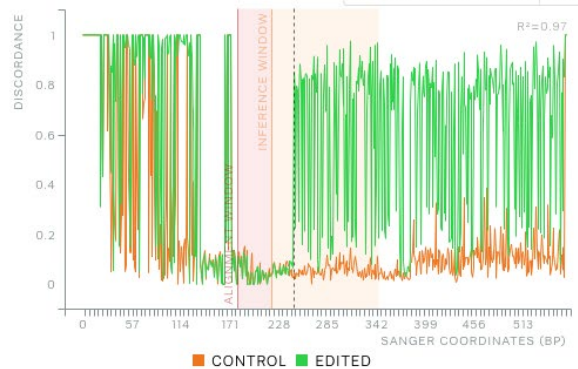
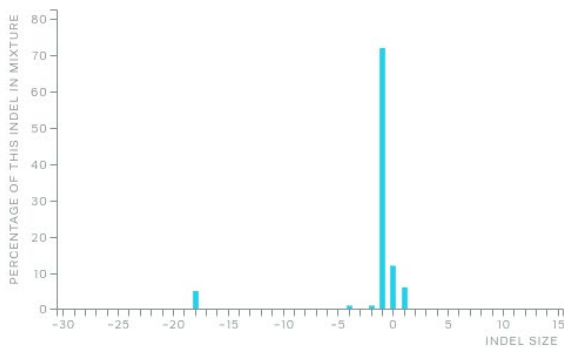
RELATIVE CONTRIBUTION OF EACH SEQUENCE (NORMALIZED)

POWERED BY SYNTHEGO ICE



The contributions show the inferred sequences present in your edited population and their relative proportions (in contrast to the Indel plot (Indel Distribution tab) that does not specify sequence contributions). Cut sites are represented by black vertical dotted lines, and the wild-type sequence is marked by a "+" symbol on the far left.

Status [?]  Succeeded <small>Padding alignment window to be at least 40bp in length or to start of seq</small>	Guide Target [?] GATTGTTGATTATTACCAAG	PAM Sequence [?] AGG	Indel % [?] 85	Model Fit (R²) [?] 0.97	Knockout-Score [?] 80
--	---	--	--	--	---



Status ②

✓ Succeeded

Padding alignment window to be at least 40bp in length or to start of seq

Guide Target ②

GATTGTTGATTATTACCAAG

PAM Sequence ②

AGG

Indel % ②

85

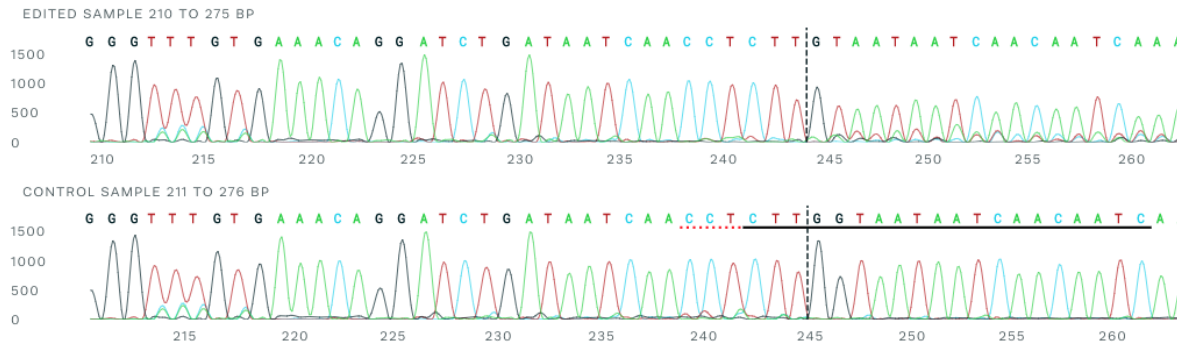
Model Fit (R²) ②

0.97

Knockout-Score ②

80

POWERED BY SYNTHEGO ICE



This is the Sanger sequence view showing edited and wild-type (control) sequences in the region around the guide sequence. This shows sequence base calls from both the control and the experimental sample .ab1 files, which will contain mixed base calls. The horizontal black underlined region represents the guide sequence. The horizontal red underline is the PAM site. The vertical black dotted line represents the actual cut site. Cutting and error-prone repair usually results in mixed sequencing bases after the cut.

Expanded UBXN2A-23971310 Knockout Cells ICE Report

Interactive results may be found here:

<https://ice.synthego.com/#/analyze/results/axayyyfmky9bv4q7/UBXN2A-23971310>

For a comprehensive guide on how to use the ICE analysis tool, check out our blog post:

<http://www.synthego.com/blog/crispr-editing-analysis-guide/>

Reference

1. Edwards G, Campbell T, Henderson V, Danaher A, Wu D, Srinivasan R, et al. SNAIL Transcription factor in prostate cancer cells promotes neurite outgrowth. *Biochimie*. 2021;180:1-9.
2. van de Wetering M, Francies HE, Francis JM, Bounova G, Iorio F, Pronk A, et al. Prospective derivation of a living organoid biobank of colorectal cancer patients. *Cell*. 2015;161(4):933-45.
3. Brembilla A, Olland A, Puyraveau M, Massard G, Mauny F, Falcoz PE. Use of the Cox regression analysis in thoracic surgical research. *Journal of thoracic disease*. 2018;10(6):3891-6.
4. Bellera CA, MacGrogan G, Debled M, de Lara CT, Brouste V, Mathoulin-Pélissier S. Variables with time-varying effects and the Cox model: some statistical concepts illustrated with a prognostic factor study in breast cancer. *BMC Med Res Methodol*. 2010;10:20.
5. van de Wetering M, Francies HE, Francis JM, Bounova G, Iorio F, Pronk A, et al. Prospective derivation of a living organoid biobank of colorectal cancer patients. *Cell*. 2015;161(4):933-45.

Supplementary Figure legends

Figure. 1S: UBXN2A negatively regulates Rictor proteins in both in vitro and patient-derived xenograft models.

A: Panel A represents a second IHC section corresponding to the mouse illustrated in Figure 1D. This section demonstrates seven high-grade adenomas based on their pathological characteristics. **B.** Panel B is a violin plot that depicts distributions of adenomas' incidence combining Low- and high-grade for WT and UBXN2A +/- mice. **C.** The Ki-67 percentage score was defined as the percentage of positively stained tumor cells among the total number of malignant cells in the prepared IHC sections. Results showed significant cell proliferation in adenomas formed in UBXN2A +/- mice versus WT mice. **D.** Panel D is photographs of xenograft tumors and their corresponding weights (**E**) used for illustrated experiments in main Fig. 2G. **F.** Panel F shows successful induction of GFP-empty and GFP-UBXN2A in xenografts by Doxycycline. **G.** Panel G demonstrates induction of GFP-UBXN2A leads to the reduction of Rictor protein in xenografts. Due to the small size of xenograft extracted from mouse 903 (UBXN2A +/-), only four mice (two WT and two UBXN2A +/-) were subjected to WB experiments. **H and I.** Tables H and I provide patients' clinical information, the status of their tumors, and received therapies used to generate patient-derived xenografts illustrated in main Figure 2 j-l. CEA, or Carcinoembryonic Antigen, is a protein marker commonly showing elevation in CRC patients and is detected in the blood. CA19-9, or Carbohydrate antigen, is a tumor marker that shows elevation in serum, particularly in patients with metastatic colon cancer.

Figure 2S: Population of GFP-Empty and GFP-UBXN2A HCT-116 cells after treatment with Doxycycline sorted by flow-cytometry analysis.

The flow-cytometry analysis illustrated in Figure 2A-D represents AKT473 or AKT308 in cells with a high level of GFP green expression. Panels A to D display the elevated expression of GFP-Empty (A versus B) or GFP-UBXN2A (C versus D) after Doxycycline treatment analyzed by flow-cytometry. As illustrated in panels C and D, we did not have many GFP-UBXN2A green cells remaining after 48 hours of induction with Doxycycline, which was expected because we normally lose some cells with a high level of UBXN2A expression due to apoptosis associated with overexpressed UBXN2A. However, the level of pAKT is dominantly decreased in GFP-UBXN2A expressing cells versus cells with GFP-Empty. We used this approach to ensure we included cells with GFP-Empty or GFP-UBXN2A.

Figure 3S: UBXN2A overexpression decreases the Rictor protein level in colon cancer cells.

A. HCT-116 TET-on GFP-empty and GFP-UBX2A cells were induced by DOX for 72 hours, and cell lysates were subjected to WB. **B.** Quantitation of Rictor signals normalized by β -actin revealed the induction of GFP-UBXN2A and not GFP alone leads to a significant reduction of Rictor protein in HCT-116 colon cancer cells ($n = 3$, mean \pm SD, *** $p < 0.001$). **C.** In another set of experiments, SW480 colon cancer cells were transiently transfected with GFP-empty or GFP-UBXN2A for 48 hours. Cells were fixed and stained with anti-Rictor polyclonal antibody and Alexa Fluor 546 fluorescent secondary antibody. SlowFade™ diamond antifade mountant with DAPI was used to stain the nucleus. Fluorescent microscopy was used to capture the protein level of Rictor in the presence of GFP-empty and GFP-UBXN2A. **D.** Quantitation of Rictor signal intensity per cell measured by ImageJ (<https://imagej.nih.gov>) revealed GFP-UBXN2A significantly decreases the protein levels of Rictor (~150 cells on triplicate slides, independently repeated three times; mean \pm SD, **** $p < 0.0001$). **E and F.** We conducted an IP experiment using a Rictor antibody (Proteintech) for IP. A polyclonal anti-Rictor antibody stabilized on magnetic IgG pull-down beads was able to pull down endogenous UBXN2A protein from HCT-116 cells.

Figure 4S: Induced apoptosis observed with overexpressed UBXN2A is associated with elevation of BAX and PUMA proteins in HCT-116 colon cancer cells.

It has been shown that the expression level of PUMA and the release of its downstream apoptotic regulators, such as BAX, are regulated in a FOXO3a-dependent manner. Furthermore, it has been reported that inhibition of mTORC2 leads to apoptosis in a FOXO3a-dependent manner, suggesting that FOXO3a activation by mTORC2 inhibitors may be a valuable chemopreventive target in cancers. Accordingly, we measured the level of early and late apoptosis in HCT-116 cells transiently transfected with DDK-empty and DDK-UBXN2A. **A-F.** Flow-cytometry analysis revealed that overexpression of DDK-UBXN2A (72 hours transient transfection) leads to a significant elevation of early (E) and late apoptosis (F). Experiments were conducted in triplicate (mean \pm SD, *** $p < 0.001$, **** $p < 0.0001$). **G.** In parallel, cell lysates of transfected cells (DDK-empty and DDK-UBXN2A) were subjected to WB. WB results show DDK-UBXN2A and not DDK-empty leads to elevation of PUMA and BAX. The WB experiments were repeated three times with similar results.

Figure 5S: UBXN2A overexpression decreases the level of VEGF in HCT-116 cells.

SW620 colon cancer cells were transiently transfected with GFP-empty or GFP-UBXN2A for 48 hours. Cells were collected, fixed, and subjected to flow cytometry analysis. Panels **A** and **C** are

nonstained GFP-empty or GFP-UBXN2A cells, respectively (negative control). Panels **B** and **D** were stained with mouse monoclonal VEGF antibody-APC. Collected data from 10000 events show a 20% reduction of VEGF in cells expressing GFP-UBXN2A. Together, the data displayed in the main Figure 5 and Figure 5S suggest that UBXN2A-dependent inhibition of the mTORC2 complex can decrease the level of VEGF protein, which is a critical factor in tumor angiogenesis.

Figure 6S: Rescue experiments with MYC-Rictor show a direct causal interaction between UBXN2A and Rictor protein in colon cancer cells.

A-C. Panels A-C show overexpression of MYC-Rictor in HCT-116 cells with induced GFP-UBXN2A can lead to a significant reduction of early apoptosis enhanced by GFP-UBXN2A (column red versus orange). Cells were incubated at time 0 with DOX for 24 hours, and then induced cells were transfected transiently with MYC-Rictor for another 48 hours. DOX treatment was maintained to the end of experiments. **D.** WB experiments in panel D revealed that elevated E-cadherin and reduced Vimentin in the presence of induced UBXN2A are reversed by overexpression of MYC-Rictor. **E-F.** Clones 3 and 9 UBXN2A KO cells were transfected with DDK-empty or DDK-UBXN2A transiently for 48 hours. WB experiments show the level of E-cadherin increases in clones 3 and 9 overexpressing DDK-UBXN2A (Lanse 4 and 5) versus low level of E-cadherin proteins in clones 3 and 9 UBXN2A KO cells (Lanse 2 and 3).

Figure 7S: Flow-cytometry analysis of LGR5 and CD133 cancer stem cell markers in HCT-116 cells overexpressing UBXN2A. HCT-116 cells were transiently transfected with DDK-empty and DDK-UBXN2A. After 48 hours, cells were collected, fixed, and subjected to flow cytometry analysis using Alexa Fluor 647 Rat Anti-Human Lgr5 (**A-F**) or APC Mouse Anti-Human CD133 (clone W6B3C1, panels **G-L**). Alexa Fluor 647 Rat IgG2b, κ Isotype (panels **B** and **E**) and APC Mouse IgG1 κ Isotype (panels **H** and **K**) were used as control along with unstained cells in panels **A**, **D**, **G**, and **J**. These sets of experiments were conducted in triplicate (see statistical analysis in main figure 7H-I).

Figure 8S: Flow-cytometry analysis of CD44 cancer stem cell marker in SW480 cells overexpressing UBXN2A.

SW480 cells were transiently transfected with DDK-empty and DDK-UBXN2A. After 48 hours, cells were collected, fixed, and subjected to flow cytometry analysis using PE Mouse Anti-Human CD44 Clone G44-26 (**A-F**). PE Mouse IgG2b κ Isotype (Panels **B** and **E**) was used as

control along with unstained cells in panels **A** and **D**. These sets of experiments were conducted in triplicate (see figure 7J).

Figure 9S: Flow-cytometry analysis of LGR5 cancer stem cell marker in SW480 cells overexpressing UBXN2A. SW480 cells were transiently transfected with DDK-empty and DDK-UBXN2A. After 48 hours, cells were collected, fixed, and subjected to flow cytometry analysis using Alexa Fluor 647 Rat Anti-Human Lgr5 (**A-F**). Alexa Fluor 647 Rat IgG2b, κ Isotype (Panels **B** and **E**) was used as control along with unstained cells in panels **A** and **D**. These sets of experiments were conducted in triplicate (see main Figure 7K).

Figure 10S: Flow-cytometry analysis of CD133 cancer stem cell marker in SW480 cells overexpressing UBXN2A. SW480 cells were transiently transfected with DDK-empty and DDK-UBXN2A. After 48 hours, cells were collected, fixed, and subjected to flow cytometry analysis using APC Mouse Anti-Human CD133 (**A-F**). APC Mouse IgG1 κ Isotype (panels **B** and **E**) were used as control along with unstained cells in panels **A** and **D**. These sets of experiments were conducted in triplicate (see figure 7L).

Figure 11S: UBXN2A induction inhibits activation of the PI3K/AKT pathway in 5-FU-resistant HCT-116 colon cancer cells.

Generated 5-FU resistant cells were incubated without and with doxycycline for 48 hours following flow cytometry for pAKT473. GFP green cells were gated before analyzing the pAKT473 signals in cells expressing GFP alone or GFP-UBXNA. The results show that UBXN2A induction can reverse chemoresistance by inhibiting the PI3K/AKT pathway.

Figure 12S: A rescue experiment shows MYC-Rictor reverses the negative regulatory impact of UBXN2A expression on colon cancer stem cells.

The GFP-Empty and GFP-UBXN2A Tet-on inducible cells treated with DOX at time 0 and maintained on DOX treatment for 72 hours. Cells were transiently transfected with MYC-Rictor 24 hours after induction with DOX for 48 Hours, followed by flow-cytometry analysis. Results indicate that induction of GFP-UBXN2A significantly decreases CD44⁺ cells in comparison to GFP-empty cells (column blue versus red). However, the level of CD44⁺ cells reversed when MYC-Rictor was overexpressed in induced GFP-UBXN2A cells (column purple versus red).